

Frequency bandwidth and potential resolution of optical modulators exploiting a multi-phonon light scattering in crystals

Alexandre S. Shcherbakov^{a,*}, Eduardo Tepichin Rodriguez^a,
Arturo Aguirre Lopez^{b,1}, Jewgenij Maximov^{c,2}

^aNational Institute for Astrophysics, Optics & Electronics, A.P. 51 y 216, Puebla 72000, Mexico

^bMixteca University of Technology, Huajuapán de León, Oaxaca 69000, Mexico

^cMolecular Technology GmbH, Rudower Chaussee 29-31 (OWZ), Berlin 12489, Germany

Received 19 October 2006; accepted 6 June 2007

Abstract

We consider physical conditions for realizing the Bragg regime of one-, two-, and three-phonon scattering of light in optically anisotropic crystalline materials. The exact and closed analytical models for describing these regimes are developed and solved. The performed analysis takes into account an opportunity of realizing 100% efficiency of light scattering in these regimes. Possible applications lie in the fields of creating large-aperture modulators of light. In connection with this, the problems of optimizing the frequency bandwidths and potential resolution of such modulators are studied. Reasonable attention is paid to the contribution of acoustic anisotropy to frequency bandwidth. The analytical results are illustrated by computer simulations and compared with proof-of-principle experimental data related to a multi-phonon light scattering in a tellurium dioxide crystal.

© 2007 Elsevier GmbH. All rights reserved.

Keywords: Non-collinear acousto-optical interaction in crystals; Multi-phonon light scattering

1. Introduction

The nonlinear behavior of light beams with Bragg acousto-optical interaction in a crystal can be easily achieved in an experiment without any observable effect of the scattering process on the acoustic wave, when the powers of the incident light and ultrasound are close to

each other and do not exceed a level of about 100 mW [1,2]. In this case, the amplitude of the acoustic wave is governed by a homogeneous wave equation, and it is agreed that the regime of so-called weak coupling takes place [3]. Here, we assume that the area of propagation for the acoustic wave, traveling almost perpendicular to the light, is bounded by two planes $x = 0$ and $x = L$ in a crystal, and initially take into account both angular and frequency mismatches in the wave vectors. Usually, the Bragg acousto-optical process includes three waves, the incident and scattered light modes as well as the acoustic mode, and incorporates conserving both the energy and the momentum for each partial act of a one-phonon light scattering. However, if the central cross-section of a pair of the wave vector surfaces, reflecting

*Corresponding author. Tel.: +52 222 266 3100x2205 or 1223; fax: +52 222 247 2940.

E-mail addresses: alex@inaoep.mx (A.S. Shcherbakov), tepichin@inaoep.mx (E. Tepichin Rodriguez), aaguirre@mixteco.utm.mx (A. Aguirre Lopez), mtberlin@aol.com (Je. Maximov).

¹Tel.: +52 953 532 0399x500; fax: +52 953 532 0214.

²Tel.: +49 30 6392 6623; fax: +49 30 6392 6622.

two eigen-states of polarization in optically anisotropic medium, is crossed by a direct line, placed close enough to a joint center of those surfaces and being collinear to the wave vector of an acoustic beam, one will obtain three or four points of intersection, see Figs. 1a and b. This fact indicates that generally the chosen geometry of acousto-optical interaction in anisotropic medium allows, as a maximum, a three-fold scattering of light by acoustic waves in the Bragg regime and in doing so represents the most complicated case of just the Bragg non-collinear interaction in crystals. In the particular case, when these four intersections are equidistant, a three-fold scattering of light can be provided by only one harmonic acoustic wave, as shown for a tellurium dioxide crystal in Fig. 1d. Then, one can consider the degenerated version for this case as well, which gives us a two-fold scattering of light, see Fig. 1c. By this it is meant that under certain conditions, i.e. at a set of angles of light incidence on selected crystal cut and at fixed frequency of the acoustic wave, one will be able to observe the Bragg scattering of light caused by sequential participation of one, two, or even three phonons. In doing so, attention can be given to searching the points of extrema for intensities of the scattered light that hold the greatest interest from the viewpoint of the light modulation technique. It is easy to show that the effects in hands are potentially suitable for realizing 100% efficiency for multi-fold light scattering via multi-phonon processes. In this paper, the feasibility of applying such a phenomenon to the modulation of light is analyzed and the problems related to optimizing the bandwidths of modulation and improving the potential resolution in these modulators are investigated theoretically, simulated numerically, and examined during proof-of-principle experiments.

The conservation laws are given by $\omega_{m+1} = \omega_m + \Omega$ and $\mathbf{k}_{m+1} = \mathbf{k}_m + \mathbf{K}$ simultaneously (ω_m , \mathbf{k}_m and Ω , \mathbf{K}

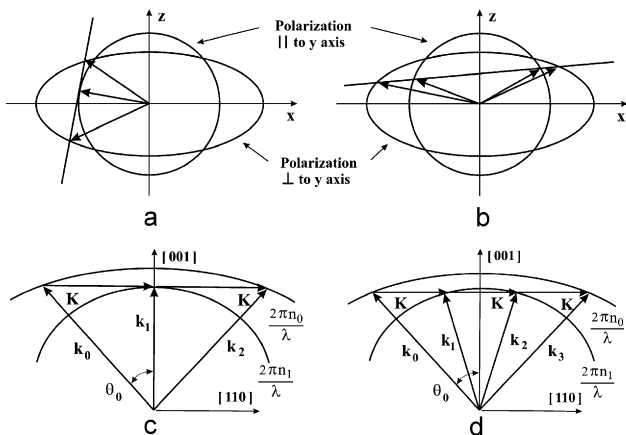


Fig. 1. Feasible geometries of acousto-optical interaction in optically anisotropic crystals: two arbitrary cases (a, b) and the particular cases of multi-phonon processes in a tellurium dioxide crystal (c, d).

are the cyclic frequencies and the wave vectors of light and acoustic waves, $m = 0, 1, 2, 3$ as the case requires). Such processes occur at various angles θ_0 of light incidence and the characteristic frequencies $\Omega_{2,3}$, peculiar to just a two- and three-fold Bragg scattering of light as

Two-fold scattering:

$$\begin{aligned} \text{(a)} \quad \sin \theta_0 &= (n_0)^{-1} \sqrt{|n_0^2 - n_1^2|}, \\ \text{(b)} \quad \Omega_2 &= 2\pi f_2 = 2\pi \lambda^{-1} V \sqrt{|n_0^2 - n_1^2|}, \end{aligned} \quad (1)$$

Three-fold scattering:

$$\begin{aligned} \text{(a)} \quad \sin \theta_0 &= 3(4n_0)^{-1} \sqrt{2|n_0^2 - n_1^2|}, \\ \text{(b)} \quad \Omega_3 &= 2\pi f_3 = \pi \lambda^{-1} V \sqrt{2|n_0^2 - n_1^2|}, \end{aligned} \quad (2)$$

where $n_0 \neq n_1$ are the refractive indices of a crystal, V is the ultrasound velocity, and λ is the incident light wavelength. The polarization states of light in various orders of scattering can be orthogonal to each other, whereas the frequencies of light beams in the first, second, and third orders are shifted by Ω_2 and $2\Omega_2$ or Ω_3 , $2\Omega_3$, and $3\Omega_3$, as the case requires, relative to the zero-order light beam, see Fig. 2.

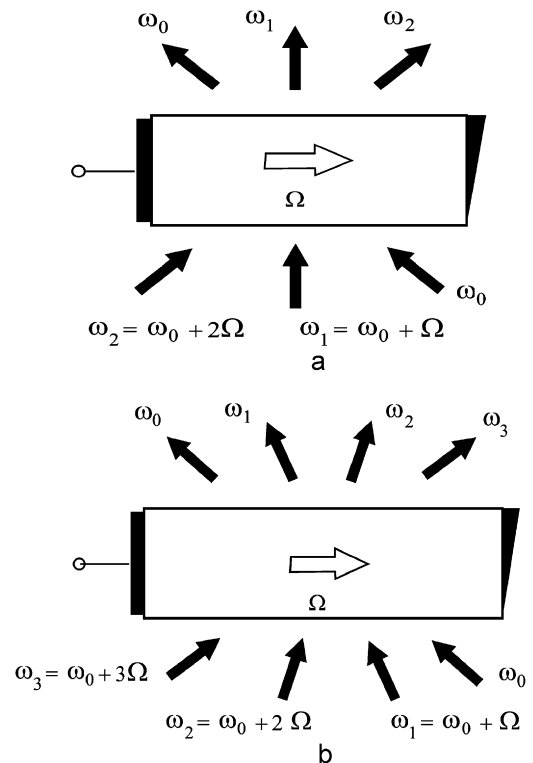


Fig. 2. Optical beam arrangements inherent in two-phonon (a) and three-phonon (b) processes of light scattering; light arrows show the corresponding acoustic waves passing through crystals from the piezoelectric transducers to the absorbers.

2. Analytical model for a multi-fold Bragg acousto-optical interaction

Here, our attention will be focused on a novel approach to the Bragg regime of N -fold, namely, a one-, two- or three-fold light scattering in optically anisotropic media [3,5] caused by multi-phonon processes, wherein the plane elastic wave with angular frequency Ω and wave number K is traveling, say, along the y -axes. Under action of such an elastic wave, the dielectric permittivity ε becomes a function of the coordinate y and time t , so it is varied as

$$\varepsilon(y, t) = \varepsilon_0 + \varepsilon_1 \sin(Ky - \Omega t + \Phi), \quad (3)$$

where ε_0 is the dielectric constant for a non-perturbed medium, ε_1 is the amplitude of variations in the dielectric constant, and Φ is the initial phase of elastic wave. The values of ε_1 and Φ are constant for a uniform plane wave. Then, let us assume that the area of propagation for the elastic wave is bounded by two planes $x = 0$ and $x = L$, and that N plane electromagnetic waves

$$E_{\text{in}} = \sum_{p=0}^N A_p \exp[i(k_p x \cos \theta_p + k_p y \sin \theta_p - \omega_p t + \varphi_p)] \quad (4)$$

strike the plane $x = 0$ at angles θ_p to the x -axis. Here $p = 0, 1, 2, \dots, N$; while A_p , φ_p , ω_p , and k_p are the normalized real amplitude, initial phase, angular frequency, and wave number of the p th incident light wave; $\omega_p = \omega_0 + p\Omega$ and $k_p = |\mathbf{k}_p| = \omega_p \varepsilon_0^{1/2} c^{-1}$. Without the loss in generality, one may state that all the fields are independent of the third coordinate. Because the directions for passing the light waves are pre-assigned by the Bragg conditions from Eqs. (1) and (2), a scalar version of the wave equation, governing the electric component $E(x, y, t)$ of electromagnetic wave in area of interaction, may be used. It would be natural to represent the project of solution in the area of $x \in [0, L]$ as a sum of partial waves with the normalized complex amplitudes $C_p(x)$, so

$$(a) \frac{\partial^2 E}{\partial x^2} + \frac{\partial^2 E}{\partial y^2} - \frac{1}{c^2} \frac{\partial^2 (\varepsilon E)}{\partial t^2} = 0, \quad (5)$$

$$(b) E = \sum_{p=0}^N C_p(x) \exp[i(k_{p,x}x + k_{p,y}y - \omega_p t)].$$

Here, $k_{p,y} = k_0 \sin \theta_0 + pK$ and $k_{p,x} = \sqrt{k_p^2 - k_{p,y}^2}$. Eq. (5b) does not contain any waves, being reflected by the dynamic acoustic grating in a medium. This may be tolerated, because usually the length for coherent interaction between co-directional waves far exceeds the same length for oppositely directed waves. Practically in experiments, each transition $\mathbf{p} \rightarrow \mathbf{p} \pm \mathbf{1}$ corresponds to only one type of scattering, normal or anomalous, and

each amplitude C_p describes only one state of polarization. In the chosen approximation, we yield

$$\frac{dC_p(x)}{dx} = q_{p-1} C_{p-1}(x) \exp[i(2\eta_{p-1}x + \Phi)] - q_{p+1} C_{p+1}(x) \exp[i(2\eta_p x + \Phi)], \quad (6)$$

$$(a) q_p = \varepsilon_1 k_p^2 (4k_{p,x} \varepsilon_0)^{-1}, \quad (b) 2\eta_p = k_{p,x} + K_x - k_{p+1,x}. \quad (7)$$

Both Eqs. (7) are explained in terms of x -components for light wave vectors. It follows from Eqs. (6) that only the neighboring pairs of orders govern the redistribution of optical energy in each p th order of scattering. When the angles θ_p of incidence for all the light beams are chosen in an arbitrary way, all the values $2\eta_p L$ far exceed π , so the scattering is not sufficiently effective. Nevertheless, for specific angles θ_p , being close to the Bragg angles, a few values $2\eta_p L$ turn out to be small, so rather effective scattering into the corresponding p th order takes place.

3. A one-fold light scattering; bandwidth of a one-phonon interaction

At first, we consider the conventional regime of a one-fold light scattering. In this case, Eqs. (6) and (7) give the well-known [4,5] set of combined equations that governs the evolution of the complex amplitudes $C_0(x)$ and $C_1(x)$ of light waves:

$$(a) \frac{dC_0}{dx} = -q_1 C_1 \exp(-2i\eta_0 x),$$

$$(b) \frac{dC_1}{dx} = q_0 C_0 \exp(2i\eta_0 x). \quad (8)$$

Using the boundary conditions $C_0(x=0) = 1$, $C_1(x=0) = 0$, and the conservation law $|C_0|^2 + |C_1|^2 = 1$, resulting from Eq. (8), one can write the solution to Eq. (8b) in terms of the scattered light intensity with $q^2 = q_0 q_1$ as

$$|C_1|^2 = \frac{q^2}{q^2 + \eta_0^2} \sin^2(x \sqrt{q^2 + \eta_0^2}). \quad (9)$$

The bandwidth of light scattering can be naturally estimated by the condition $\sqrt{(qx)^2 + (\eta_0 x)^2} = \pi/2$, corresponding to a level of about -4 dB for the sinus function in Eq. (9). It follows from this condition that an acceptable magnitude of the normalized mismatch $\eta_0 x$ decreases as the parameter qx grows. Formally speaking, the bandwidth cannot be determined correctly by this condition with $qx \geq \pi/2$. In fact, however, we have to restrict the normalized mismatch by the stronger inequality $qx \leq \pi/2$ due to the unacceptable level of the side lobes in the intensity distribution with $qx \geq \pi/2$. This is illustrated in Fig. 3 by a three-dimensional intensity

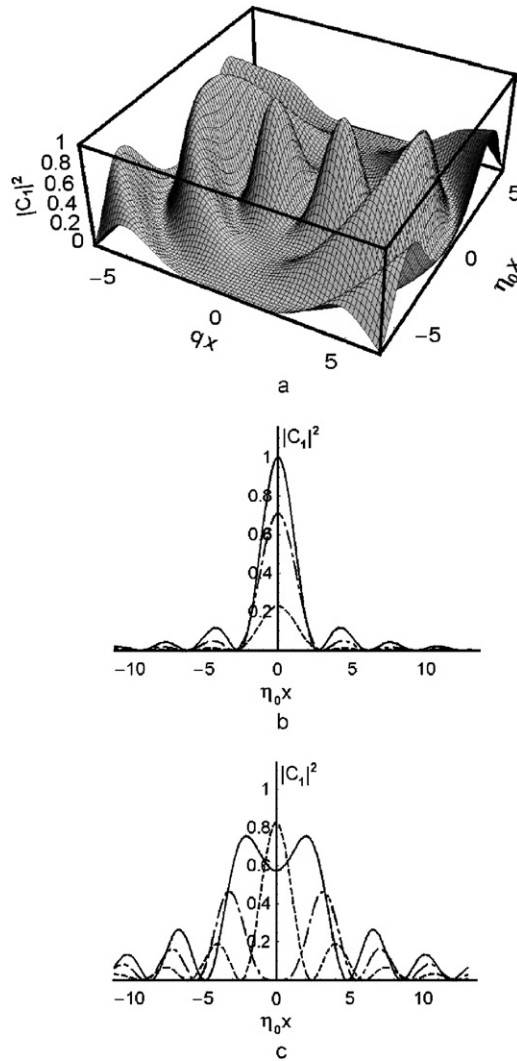


Fig. 3. A three-dimensional intensity distribution (a) for $|C_1(qx, \eta_0x)|^2$ and two cross-sections of the light intensity distribution with two sets of fixed parameters qx versus the normalized mismatch η_0x ; (b) the region $qx \leq \pi/2$ (dashed line is for $qx = 0.5$, dot-dashed line is for $qx = 1.0$, and solid line is for $qx = \pi/2$), when the bandwidth can be well identified independently of the value of qx for an arbitrary magnitude of η_0x ; (c) the region of $\pi/2 < qx \leq \pi$ (dashed line is for $qx = 2$, dot-dashed is line for $qx = \pi$, and solid line is for $qx = 4$), when the bandwidth cannot be always determined correctly.

distribution for $|C_1(qx, \eta_0x)|^2$ and a pair of cross-sections of this distribution. The set of plots in Figs. 3 obviously demonstrates that it is simpler to use the concept of a small signal bandwidth. It can be estimated with $q \rightarrow 0$ from the previous equality, which takes now the form of $\eta_0x = \pi/2$.

A one-phonon non-collinear light scattering in isotropic medium is associated with the Bragg condition [4,5]

$$\sin \theta = -K/(2k_0) = -\lambda f_1/(2nV) \tag{10}$$

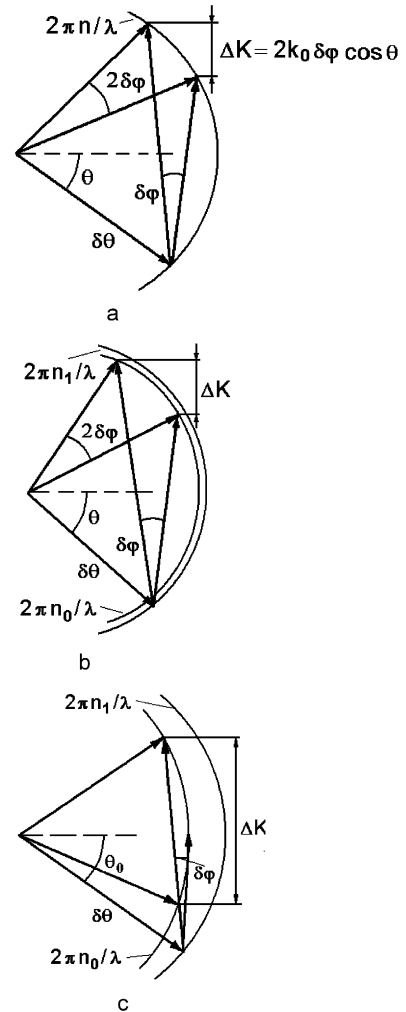


Fig. 4. Vector diagram related to the bandwidths of the normal scattering (a), the non-optimized anomalous scattering (b) with $\zeta \rightarrow 0$, and the optimized anomalous scattering (c) with $\zeta \neq 0$.

for the normal regime without changing the state of light polarization. The corresponding wave vector diagram is depicted in Fig. 4a. The frequency bandwidth of acousto-optical interaction Δf_1 can be estimated through differentiating this Bragg condition in Eq. (10) as $\Delta f_1 = \Delta\theta(2nV/\lambda) \cos \theta$, where $\Delta\theta$ is the variation of the angle of light incidence associated with the variation of the acoustic frequency Δf_1 needed to provide the Bragg condition. In the case of light modulation, we usually have the geometry of interaction with a rather wide optical beam, whose angle of spreading $\delta\theta$ is small, and a rather narrow aperture of the acoustic beam (i.e. a rather large size L_T of the piezoelectric transducer), whose angle of spreading is $\delta\varphi \approx (V/f_1 L_T) \gg \delta\theta$ in the case of ordinary acoustic beam diffraction in an isotropic medium. Assuming that $\delta\varphi \approx \Delta\theta$, $L_T \approx L$, and $\cos \theta \approx 1$, we obtain the following rather good

approximations:

$$(a) \Delta f_1 \approx \frac{2nV^2}{\lambda L f_1}, \quad (b) \Delta f_1 \approx \frac{2nV}{\lambda} \delta\varphi, \quad (11)$$

for the bandwidth of normal Bragg acousto-optical interaction in an isotropic medium. This approximate equality follows geometrically from the plot in Fig. 4a, because $\Delta K = 2\pi(\Delta f_1)/V$ and $2k_0\delta\varphi \cos \theta \approx 4\pi nV/(\lambda L f_1)$. Moreover, in the case of normal one-phonon light scattering, Eq. (7b) together with Fig. 3a give us $\eta_0 = \pi\lambda f_1(\Delta f_1)/(2nV^2)$. Using the equality $\eta_0 x = \pi/2$ with $x = L$, one can obtain Eq. (11a) again.

The regime of a one-phonon anomalous non-collinear light scattering in a slightly anisotropic medium, when the state of light polarization becomes changed via the scattering process, is characterized by the modified Bragg condition [6]:

$$(a) \sin \theta_{0,1} = \frac{\lambda f}{2n_{0,1}V} \left(1 \pm \frac{V^2 \zeta^2}{\lambda^2 f^2}\right), \quad (b) \zeta^2 = n_0^2 - n_1^2, \quad (12)$$

where $n_{0,1}$ are the refractive indices. In the frames of this regime, two different cases can be recognized here. The first case of a non-optimized one-phonon non-collinear anomalous light scattering can be associated with an approximation of $\zeta = 0$ due to rather small birefringence; it is presented in Fig. 4b. Comparing Figs. 4a and b, one can see that in fact these two plots are very close to each other. That is why one can suppose that, if the birefringence is small enough in an anisotropic medium, the same approximation, i.e. just Δf_1 , may be approximately applied to estimate the bandwidth of acousto-optical interaction in an anomalous Bragg regime with a one-phonon non-collinear light scattering. Together with that, in the second case, a one-phonon non-collinear light scattering in anisotropic medium can be optimized with $\zeta \neq 0$ due to choosing the special acoustic frequency $f_0 = V\zeta/\lambda$, which corresponds to the absolute minimum of the function $\theta_0(f)$ on the frequency interval $f \in [0, f_{\max} = V\lambda^{-1}(n_0 + n_1)]$. On the one hand, substituting such a special acoustic frequency in the modified Bragg condition, see Eq. (12), differentiating Eq. (12) with respect to frequency f , and using an expansion into a power series, one can obtain the frequency bandwidth

$$(a) \Delta f_0 \approx 2V\sqrt{2n_0/(\lambda L)}, \quad (b) \Delta f_0 \approx 2V\sqrt{2n_0\zeta\lambda^{-1}\delta\varphi}, \quad (13)$$

for the optimized geometry of a one-phonon non-collinear anomalous acousto-optical interaction, which is shown schematically in Fig. 4c. On the other hand, in the case of anomalous one-phonon light scattering, Eq. (7b) together with Fig. 3c give us $\eta_0 = \pi\lambda(\Delta f_0)^2/(2nV^2)$. Using again the equality $\eta_0 x = \pi/2$ with $x = L$, one can obtain Eq. (13a) as well. Then, the following

ratio $\Delta f_0/\Delta f_1 = \sqrt{2L\zeta^2/(\lambda n_0)} > 1$ can be constructed to compare normal and anomalous regimes. This ratio determines an advantage of applying the optimized anomalous process to light modulation in comparison with normal one from the viewpoint of the bandwidth for light scattering.

4. Two-fold light scattering; bandwidth of a two-phonon interaction

Using the Eqs. (6) and (7), one can obtain the evolution equations describing a two-fold light scattering as well. In the case of a two-fold light scattering presented in Fig. 1c, Eq. (6) can be considerably simplified because one can disregard all the amplitudes $C_p(x)$ in Eq. (6) with the exception of the amplitudes C_0 , C_1 , and C_2 , so that

$$(a) \frac{dC_0(x)}{dx} = -q_1 C_1(x)\exp(-2i\eta_0 x),$$

$$(b) \frac{dC_1(x)}{dx} = q_0 C_0(x)\exp(2i\eta_0 x) - q_2 C_2(x)\exp(-2i\eta_1 x),$$

$$(c) \frac{dC_2(x)}{dx} = q_1 C_1(x)\exp(2i\eta_1 x). \quad (14)$$

It may be tolerated on the above-mentioned assumption that the shifts in carrier angular frequencies of light waves, included in the amplitude coefficients for different orders, can be neglected. All the parameters q_p with $p = 0, 1, 2$ describe the efficiency of interaction with changing the state of light polarization, and what is more, these two steps of scatterings are provided by the same photo-elastic constants. That is why one can put $q_0 = q_1 = q_2 \equiv q$. We analyze Eqs. (14) with the simplest boundary conditions $|C_0(x=0)|^2 = 1$ and $C_{1,2}(x=0) = 0$. The exact solution to Eqs. (14) related to $C_2(x)$ in this regime [7] can be written in a reasonable format as

$$C_2(x) = iq^2 \left\{ \frac{1 - \exp[i(2\eta - a_0)x]}{(a_0 - a_1)(a_0 - a_2)} + \frac{1 - \exp[i(2\eta - a_1)x]}{(a_2 - a_1)(a_0 - a_1)} - \frac{1 - \exp[i(2\eta - a_2)x]}{(a_2 - a_1)(a_0 - a_2)} \right\}. \quad (15)$$

Here, a_m are roots of the cubic equation $a^3 - 2(\eta_0 + \eta)a^2 - (2q^2 - 4\eta\eta_0)a + 2q^2\eta = 0$ and $\eta = \eta_0 + \eta_1$. Generally, as it follows from Eq. (15), the intensity of this scattered light wave $|C_2(x)|^2$ is periodic in x . When $\eta_0 = \eta_1 = 0$, one can obtain $a_0 = 0$ and $a_{1,2} = \pm q\sqrt{2}$, so that $C_2(x) = \sin^2(qx/\sqrt{2})$. Consequently, in this case of the exact phase synchronism, even 100% of the incident light can be scattered into the second order at $qx = \pi/\sqrt{2}$.

Now, we assume a precise angular alignment and extend η_0 and η_1 into a series in terms of the only frequency detuning $f - f_2$ for the current frequency f

relative to the central frequency f_2 determined by Eq. (1b). In the second approximation with respect to $f-f_2$, one can obtain from Eq. (7b) and the diagram of wave vectors in Fig. 1c that [4]

$$\begin{aligned} \text{(a)} \quad 2\eta_0 &\approx -\pi\lambda n_0^{-1} V^{-2}(f-f_2)^2, \\ \text{(b)} \quad 2\eta_1 &\approx -4\pi\lambda n_0^{-1} V^{-2}f_2(f-f_2) \\ &\quad -7\pi\lambda n_0^{-1} V^{-2}(f-f_2)^2. \end{aligned} \quad (16)$$

Consequently, in the first approximation with respect to $f-f_2$, we obtain

$$\text{(a)} \quad \eta_0 \approx 0, \quad \text{(b)} \quad \eta_1 \approx -2\pi\lambda n_0^{-1} V^{-2}f_2(f-f_2). \quad (17)$$

Exploiting Eq. (17) for the sake of simplicity and substituting Eq. (17) into Eq. (14), one can draw a three-dimensional distribution for $|C_2(x)|^2$, see Fig. 5a, and estimate the dependence of light intensity $|C_2(x)|^2$ on the product $\eta_1 x$, where the mismatch η_1 is connected with the frequency detuning $(f-f_2) \approx \eta_1 n_0 V^2 (2\pi\lambda f_2)^{-1}$. It is seen from Fig. 5a that the first maxima of unity level in this distribution can be reached at $qx = \pm\pi/\sqrt{2}$. At the same time, by analogy with the previous section, one should take $\eta_1 x = \pi/2$ with $x = L$, see Fig. 5b, to find the bandwidth $\Delta f_2 = 2(f-f_2)$ of a two-phonon light scattering:

$$\text{(a)} \quad \Delta f_2 \approx \frac{n_0 V^2}{2\lambda f_2 L}, \quad \text{(b)} \quad \Delta f_2 \approx \frac{n_0 V}{2\lambda} \delta\varphi. \quad (18)$$

The comparison of this formula with Eq. (11) makes it possible to conclude that the bandwidth of a two-

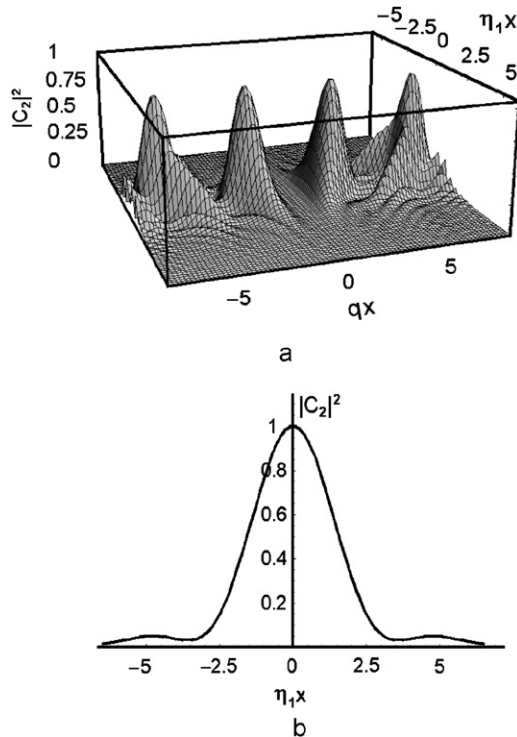


Fig. 5. A three-dimensional distribution (a) for $|C_2(qx, \eta_1 x)|^2$ and (b) the cross-section of that distribution at $qx = \pi/\sqrt{2}$.

phonon light scattering is about four times narrower than a bandwidth of the normal one-phonon scattering.

5. A three-fold light scattering; a simplified estimation for the bandwidth of a three-phonon interaction

Now we can disregard all the amplitudes $C_p(x)$ in Eq. (6) with the exception of the amplitudes C_0 , C_1 , C_2 , and C_3 , as shown in Fig. 1d, and, in so doing, obtain the following set of only four simplified ordinary differential equations for complex amplitudes of the scattered light waves:

$$\begin{aligned} \text{(a)} \quad \frac{dC_0(x)}{dx} &= -q_1 C_1(x) \exp(-2i\eta_0 x), \\ \text{(b)} \quad \frac{dC_1(x)}{dx} &= q_0 C_0(x) \exp(2i\eta_0 x) - \tilde{q}_2 C_2(x) \exp(-2i\eta_1 x), \\ \text{(c)} \quad \frac{dC_2(x)}{dx} &= \tilde{q}_1 C_1(x) \exp(2i\eta_1 x) - q_3 C_3(x) \exp(-2i\eta_2 x), \\ \text{(d)} \quad \frac{dC_3(x)}{dx} &= q_2 C_2(x) \exp(2i\eta_2 x). \end{aligned} \quad (19)$$

In Eqs. (19), the parameters q_p ($p = 0, 1, 2, 3$) can be rewritten in terms of normal and anomalous scattering of light in a uniaxial crystal as $\tilde{q}_1 = \tilde{q}_2 = q_n$ and $q_0 = q_3 = q_a$. The factors q_n and q_a describe both the material properties relative to normal and anomalous processes of light scattering and the acoustic power density, and they can be taken to be constants. Generally, $q_n \neq q_a$, because these factors include different components of the photo-elastic tensor inherent in a crystal.

Now, we again assume a precise angular alignment and extend η_0 , η_1 , and η_2 into a series in terms of the only frequency detuning $f-f_3$ for the current frequency f relative to the central frequency f_3 determined by Eq. (2b). In the first approximation with respect to $f-f_3$, one can obtain from Eq. (7b) and the diagram of wave vectors in Fig. 1d that [4]

$$\begin{aligned} \text{(a)} \quad 2\eta_0 &\approx \pi\lambda n_0^{-1} V^{-2}f_3(f-f_3), \\ \text{(b)} \quad \eta_1 &\approx -3\eta_0, \\ \text{(c)} \quad \eta_2 &\approx -7\eta_0. \end{aligned} \quad (20)$$

Varying the ratio $q = q_a/q_n$ and substituting Eq. (20) into Eq. (19), one can estimate the dependence of light intensity $|C_3(x)|^2$ on the product $q_n x$. The plots in Fig. 6a show that the ratio $q = q_a/q_n$ should be optimized from the viewpoint of applications to light modulation. The best value of this ratio $q = 0.866$ provides the monotonic character of increasing the light intensity $|C_3(x)|^2$ and an opportunity of reaching the 100% maximum intensity at $q_n x = \pi$, see the solid line in Fig. 6a. A similar possibility exists for the ratio $q = 1.936$, but it gives a non-monotonic character of

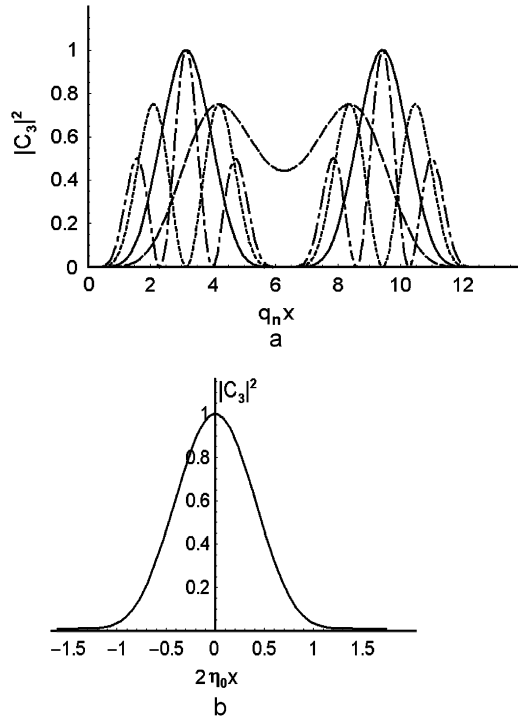


Fig. 6. Distributions of the light intensity $|C_3(x)|^2$. Here, (a) the dependences on the product $q_n x$: dashed line is for $q_n = 0.559$, solid line is for $q_n = 0.866$, dotted line is for $q_n = 1.414$, and dot-dashed line is for $q_n = 1.936$. (b) The dependence on the product $2\eta_0 x$: $q_n x = \pi$ and $q = 0.866$.

increasing the light intensity $|C_3(x)|^2$ with $q_n x$, see the dot-dashed line in Fig. 6a. Then, in the case of $q_n x = \pi$, one can consider the dependence of the light intensity $|C_3(x)|^2$ on the product $2\eta_0 x$, see Fig. 6b, where η_0 is connected with the frequency detuning $f - f_3 \approx 2\eta_0 n_0 V^2 (\pi \lambda f_3)^{-1}$. By analogy with the previous sections, one has to take $2\eta_0 x \approx \pi/6$ at $x = L$. Such a selection makes it possible to find the expression

$$\begin{aligned} \text{(a)} \quad \Delta f_3 &= 2(f - f_3) \approx \frac{n_0 V^2}{3\lambda f_3 L}, \\ \text{(b)} \quad \Delta f_3 &\approx \frac{n_0 V}{3\lambda} \delta\varphi, \end{aligned} \quad (21)$$

for the bandwidth of a three-phonon light scattering with $q = 0.866$. Finally, the value of Δf_3 is approximately six times less than the bandwidth Δf_1 of a one-phonon light scattering in normal regime, described by Eq. (11).

6. Potential resolution of the modulators under consideration

Potential resolution of acousto-optical modulator has the same physical nature as the resolution of conventional diffractive grating in optics, because an acousto-optical cell represents in fact a dynamic acoustic grating

inside the cell's material. To estimate the resolution of an optical modulator let us use the quantum mechanical approach. Generally, the momentum p of a photon is connected with the wave number k as $p = \hbar k / (2\pi)$, where \hbar is the Planck constant, so an uncertainty $\delta p = \hbar(\delta k) / (2\pi)$ in the momentum is related to the uncertainty in the wave number δk of a photon. The same view is true, if one will consider the phonons. Namely, the momentum P of a phonon is connected with the wave number K as $P = \hbar K / (2\pi)$, and an uncertainty $\delta P = \hbar(\delta K) / (2\pi)$ in the momentum is related to the uncertainty in the wave number δK of a phonon. Then, because the phonon wave number is $K = 2\pi f / V$, one can note that an uncertainty of the phonon wave number, in its turn, can be explained in terms of an uncertainty in the phonon frequency δf as $\delta K = 2\pi(\delta f) / V$. The limiting case of just Bragg light scattering in acousto-optics is determined by the well-known [8] dimensionless inequality $\lambda f^2 L / V^2 \gg 1$. In this limit an uncertainty in the momentum of the issuing photon is characterized by the relation $\delta p \approx \delta P$, and, consequently, $\delta k \approx \delta K$, because they both are localized inside the same spatial area determined by the aperture D . Together with this, the value of δk is significantly smaller than the photon wave number variation connected with scattering from the order j to the order $j+1$, i.e. $|\mathbf{k}_{j+1} - \mathbf{k}_j| \gg K \gg \delta K \gg \delta k$. By this, it is meant that the wave numbers of both the photons and the phonons are well determined in the Bragg limit of acousto-optical interaction. Due to the Heisenberg uncertainty principle [9] proclaiming that $\delta p \cdot \delta x \sim \hbar$ with $\delta x \approx D$, one can find that

$$\delta f \approx V / D. \quad (22)$$

Just this value determines the potential frequency resolution of acousto-optical modulators independently of the number of phonons taking part in a process of the Bragg light scattering.

Eq. (22) gives us an opportunity to estimate the number $N_m = \Delta f_m / \delta f$ of resolvable spots for each of the modulators under analysis. In so doing and using Eqs. (11a), (13a), (18a), and (21a) together with Eq. (22), one can calculate for a one-phonon (normal as well as the anomalous optimized), two-phonon, and three-phonon processes of light scattering

$$\begin{aligned} \text{(a)} \quad N_1 &= \frac{2nVD}{\lambda f_1 L}, & \text{(b)} \quad N_0 &= 2D \sqrt{\frac{2n_0}{\lambda L}}, \\ \text{(c)} \quad N_2 &= \frac{n_0 VD}{2\lambda f_2 L}, & \text{(d)} \quad N_3 &= \frac{n_0 VD}{3\lambda f_3 L}. \end{aligned} \quad (23)$$

Then, one can consider the angular resolution of these acousto-optical modulators. For simplicity sake, let us omit for a moment the optimized anomalous regime and take the angular-frequency dependences in the forms

$$\sin \theta_m = \frac{m}{2} \frac{K}{k_m} = \frac{m}{2} \frac{\lambda f_m}{n_0 V}, \quad (24)$$

which are true within the limits of the corresponding bandwidths Δf_m . These equations directly follow from Fig. 4a for $m = 1$, Fig. 1c for $m = 2$, and Fig. 1d for $m = 3$. It is easy to find from Eq. (24) that small variations $\text{var}\theta_m$ of the angles θ_m are connected with the corresponding variations $\text{var}f_m$ of the frequencies f_m as

$$\text{var}\theta_m = \frac{m\lambda}{2n_0V\cos\theta_m}\text{var}f_m. \quad (25)$$

The angular size of a resolvable spot is determined by the width of the light beam or the modulator's aperture D as $\delta\theta \approx \lambda/(n_0D)$. Using this ratio, one can estimate the number of resolvable spots M_m located inside a two-side small angular interval of variation as

$$M_m = \frac{2\text{var}\theta_m}{\delta\theta} = m\left(\frac{D}{V\cos\theta_m}\right)\text{var}f_m, \quad (26)$$

where practically $\cos\theta_m \approx 1$. In Eq. (26), the term $T = D/V\cos\theta_m$ describes the time of scanning the light beam through just one resolvable spot, i.e. characterizes the speed of a modulator's operation. Among other things, one can state that values of the variations $\text{var}f_m$ are the same for all $m = (1, 2, 3)$. In this particular case, Eq. (26) shows that one and the same modulator operating in one and the same frequency bandwidth provides the number of resolvable spots directly proportional to the number m of phonons taking part in the light scattering process. In other words, the exploitation of a two- and/or three-phonon light scattering provides the increasing specific resolution of modulators under consideration. Taking alone the regime of a one-phonon light scattering with ($m = 1$) and choosing $\text{var}f_1 = \Delta f_1$, one can derive the equivalence between Eqs. (26) and (23a). When $m = (2, 3)$, the corresponding relations become more complicated due to additional restrictions within the varying wave vectors on the diagrams in Figs. 1c and d. These restrictions are ultimately conditioned by the necessity of meeting the conservation laws at all the intermediate stages of multi-phonon light scattering.

7. Effect of acoustic anisotropy

For our experiments with multi-phonon processes, we have selected a well-known and very effective acousto-optic material such as the tellurium dioxide single crystal [10], which is very anisotropic in behavior. Its acoustic anisotropy can be illustrated, for example, by one of the cross-sections of a three-dimensional surface for the acoustic waves phase velocities in TeO_2 by the $(1\bar{1}0)$ -plane [11], see Fig. 7. One can see that the slow shear acoustic mode, which is marked as the M_2 -mode in Fig. 7, has the absolute minimum ($V = 0.616 \times 10^5$ cm/s) on passing along the $[110]$ or $[1\bar{1}0]$ axes due to a tetragonal symmetry of a TeO_2 -crystal.

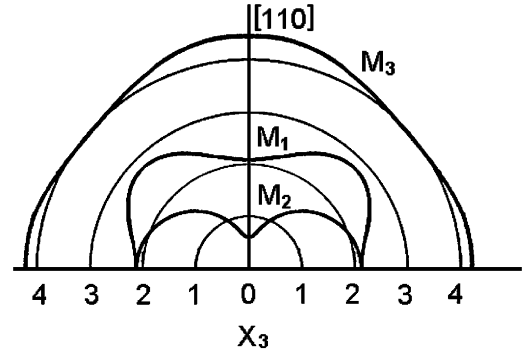


Fig. 7. Cross-section of a surface for the acoustic waves phase velocities by the $(1\bar{1}0)$ -plane in a TeO_2 crystal; the velocities are measured in 1×10^5 cm/s.

Generally, when an elastic (acoustic) wave passes through an anisotropic medium, the energy flow tips out of the wave vector $\mathbf{K} = (2\pi/\Lambda)\mathbf{m} = K\mathbf{m}$, where Λ is the acoustic wavelength and \mathbf{m} is the unit vector of the wave normal. Velocity and direction of passing the energy flow are characterized by the group velocity vector $\mathbf{w} = \partial\Omega/\partial\mathbf{K} = w\mathbf{s}$, where \mathbf{s} is the unit vector of the energy flow. The scalar product $\mathbf{w} \cdot \mathbf{m} = V$ shows that $w \geq V$, and the acoustic group velocity w is equal to the phase velocity V only if $\mathbf{s} \parallel \mathbf{m}$. The angle Ψ between the flow vector \mathbf{w} and the wave vector \mathbf{K} is determined by $\cos\Psi = \mathbf{m} \cdot \mathbf{s}$, and it can reach rather large values, of the order of tens of degrees, in the acoustically anisotropic crystals.

Now, let us discuss the dependence of w on the length K of the wave vector \mathbf{K} and its unit vector \mathbf{m} . One can write in the form of vector components that

$$w_i = \frac{\partial\Omega}{\partial K_i} = \frac{\partial\Omega}{\partial K} \frac{\partial K}{\partial K_i} + \frac{\partial\Omega}{\partial m_j} \frac{\partial m_j}{\partial K_i}. \quad (27)$$

A triplet of the orthogonal axes $\{x, y, z\}$ for a crystal (in this section) can be chosen in Eq. (27) in various ways; in particular, one can state that this triplet includes the crystallographic axes $\{[001], [110], [1\bar{1}0]\}$, respectively. Because $\Omega = VK$, one can obtain $\partial\Omega/\partial K = V$ and $\partial\Omega/\partial m_j = K(\partial V/\partial m_j)$. The other derivatives are

$$\begin{aligned} \frac{\partial K}{\partial K_i} &= \frac{\partial\sqrt{K_i K_i}}{\partial K_i} = \frac{K_i}{K} = m_i, \\ \frac{\partial m_j}{\partial K_i} &= \frac{\partial(K_j/K)}{\partial K_i} = \frac{1}{K^2} \left(K \frac{\partial K_j}{\partial K_i} - \frac{\partial K}{\partial K_i} K_j \right) \\ &= \frac{1}{K} (\delta_{ij} - m_i m_j). \end{aligned} \quad (28)$$

Substituting Eqs. (28) into Eq. (27), one can obtain in the vector components (a) as well as in the vector form (b) that

$$w_i = Vm_i + (\delta_{ij} - m_i m_j) \frac{\partial V}{\partial m_j}, \quad \mathbf{w} = V\mathbf{m} + (I - \mathbf{m}\mathbf{m}) \frac{\partial V}{\partial \mathbf{m}}. \quad (29)$$

Thus, the group velocity vector \mathbf{w} can be represented as a sum of the phase velocity vector $V\mathbf{m}$ and a part of the derivative $\partial V/\partial \mathbf{m}$, which is orthogonal to the unit vector \mathbf{m} of wave normal. Together with this, Eq. (29) is associated with the two following equalities: the first for the scalar product ($\mathbf{m} \cdot \mathbf{m} = 1$), conditioned by normalizing the unit vector \mathbf{m} , and the second for the above-mentioned product $\mathbf{w} \cdot \mathbf{m} = V$, because $(\delta - \mathbf{m}\mathbf{m}) \cdot (\partial V/\partial \mathbf{m}) \perp \mathbf{m}$. Eq. (29) give that $s \parallel \mathbf{m}$ at the points where $\partial V/\partial \mathbf{m} = 0$, for example, at a direction of the $[1\ 1\ 0]$ -axis. Together with this, Eq. (29) shows that the more the flow vector \mathbf{w} tips out of the wave vector \mathbf{K} , the more the phase velocity V varies with the direction \mathbf{m} due to $\partial V/\partial \mathbf{m} \neq 0$ with such a variation, so the angle $\Psi = \arccos(\mathbf{m} \cdot \mathbf{s})$ goes from zero. Then, Eq. (29) predicts that the faster the phase velocity varies with \mathbf{m} , the farther the vector \mathbf{w} tips from the vector \mathbf{K} . Moreover, the vector \mathbf{w} tips in a direction of the increasing velocity, i.e. just outside of a point of a minimal value of the phase velocity in a TeO_2 -crystal. That is why, in its turn, the presence of even small tips of the vector \mathbf{m} from the $[1\ \bar{1}\ 0]$ -axis in that crystal, which can be governed, for example, by diffraction of the acoustic waves and the corresponding spreading of an angular spectrum of the plane waves generated initially by a piezoelectric transducer due to its finite length L , leads immediately to the appearance of the above-noted tips of the vector \mathbf{w} . As a result, to estimate angular distribution of the acoustic energy in a crystal one has to take into account an additional two-side angular contribution 2Ψ , caused by the anisotropy of a crystal, together with the previously introduced contribution $\delta\varphi$, caused by the diffraction.

To estimate this phenomenon one can exploit Eq. (29). Let us assume that \mathbf{m} lies in the $(1\ \bar{1}\ 0)$ -plane ($|\mathbf{m}| = 1$) and α is the angle between the wave normal \mathbf{m} and the $[1\ 1\ 0]$ -axis. In this case, $\partial V/\partial m_j = (\partial V/\partial \alpha)(\partial \alpha/\partial m_j)$ in Eq. (29a) and $m_x = \sin \alpha$, $m_y = \cos \alpha$, $dm_x/d\alpha = \cos \alpha$, $dm_y/d\alpha = -\sin \alpha$, so that $d\alpha/dm_x = 1/\cos \alpha$ and $d\alpha/dm_y = -1/\sin \alpha$. Now, let us find the dependence of the phase velocity V on the angle α , see Fig. 8.

We assume that, when α is small enough, an area in the vicinity of the local minimum for the phase velocity

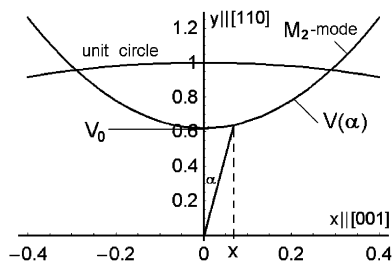


Fig. 8. Parabolic approximation of the phase velocity V for the slow shear M_2 -mode in the vicinity of the $[1\ 1\ 0]$ -axis in a TeO_2 crystal, see Fig. 7.

V at the $[1\ 1\ 0]$ -axis in the TeO_2 -crystal for the M_2 -mode in Fig. 7 can be approximated by the parabolic profile $V = V_0 + \beta x^2$, where β is a factor to be found. Together with this, it follows from Fig. 8 that $x = V \sin \alpha$. Combining these two expressions, one can write the algebraic equation $V = V_0 + \beta V^2 \sin^2 \alpha$. Only one of the solutions to this algebraic equation has physical meaning. It takes the form $V \approx V_0 + \beta V_0^2 \sin^2 \alpha$ and describes the needed dependence of the phase velocity V on the angle α . A similar solution can be calculated with the usage of the extension $\sqrt{1-z} \approx 1 - (z/2) - (z^2/8)$ in the second approximation. After that, one can find the derivative $\partial V/\partial \alpha = 2\beta V_0^2 \sin \alpha \cos \alpha$. Using this formula together with previous ones, one can calculate

$$(a) \frac{\partial V}{\partial m_x} = 2\beta V_0^2 \sin \alpha, \quad (b) \frac{\partial V}{\partial m_y} = -2\beta V_0^2 \cos \alpha. \quad (30)$$

Then, applying Eq. (29a), one can obtain

$$(a) w_x = V_0 \sin \alpha + 4\beta V_0^2 \sin \alpha \cos^2 \alpha, \quad (b) w_y = V_0 \sin \alpha - 4\beta V_0^2 \sin^2 \alpha \cos \alpha. \quad (31)$$

The length w of the vector \mathbf{w} can be found as $w = \sqrt{w_x^2 + w_y^2} = V_0 \sqrt{1 + 4\beta^2 V_0^2 \sin^2(2\alpha)}$, where $4\beta^2 V_0^2 \sin^2(2\alpha) \ll 1$ due to the expected smallness of the angle α . Using this formula, one can estimate

$$\cos \Psi = \mathbf{m} \cdot \mathbf{s} = \mathbf{m} \cdot \frac{\mathbf{w}}{w} = \frac{1}{\sqrt{1 + 4\beta^2 V_0^2 \sin^2(2\alpha)}}. \quad (32)$$

Because the angle Ψ is expected to be rather small as well as α , Eq. (32) can be reduced in the second approximation at $\cos \Psi \approx 1 - (\Psi^2/2) \approx 1 + 2\beta^2 V_0^2 \sin^2(2\alpha) \approx 1 + 8\beta^2 V_0^2 \alpha^2$. Thus finally, one can obtain

$$\Psi \approx 4\beta V_0 \alpha. \quad (33)$$

The above-mentioned parabolic approximation $V = V_0 + \beta x^2$ for the M_2 -mode in the vicinity of the local minimum for the phase velocity V at the $[1\ 1\ 0]$ -axis in TeO_2 -crystal gives the best result when the factor β is chosen to be close to $\beta = 5$. In so doing, one can estimate from Eq. (33) that, in the particular case of $V_0 = 0.616$, we obtain $\Psi \approx 12.3\alpha$. In an acousto-optical cell, in fact, the angle α is equal to the half of a two-side angle $\delta\varphi$ of spreading the acoustic beam in a cell. That is why, to take into account the effect of acoustic anisotropy, one should substitute the angle $\delta\varphi$ in Eqs. (11b), (13b), (18b), and (21b) by the enlarged value of $(2 \times 12.3 + 1)\delta\varphi \approx 25.6\delta\varphi$, because the contribution from the acoustic anisotropy significantly (about 20 times) exceeds the contribution from the acoustic diffraction.

8. Estimations and experimental results

It is worthwhile for our purposes to begin the consideration from a few practical estimations. We have selected a tellurium dioxide single crystal as a material for the acousto-optical cell. This crystal has a rather dispersive refractive index n_0 , whose values are equal to $n_0 = 2.26$ at $\lambda = 633$ nm, $n_0 = 2.33$ at $\lambda = 488$ nm and $n_0 = 2.35$ at $\lambda = 442$ nm [12], and the ultrasound velocity $V = 0.616 \times 10^5$ cm/s for the slow shear acoustic mode running along the $[1\bar{1}0]$ -axis with the displacement vector directed along the $[110]$ -axis [12], see Section 7. The figure of acousto-optical merit for this shear mode wave in a TeO_2 -crystal is $M_2 \approx 1200 \times 10^{-18}$ s³/g [10,12], the most for solid-state acousto-optical materials in the visible range. At first, we have to check the realization of just the Bragg regime for light scattering in the chosen cell. In such a regime, the Klein–Cook parameter $Q = \lambda L f^2 / (nV^2)$ [8] should exceed unity. Operating at the light-blue optical wavelength $\lambda = 448$ nm and at the lowest expected acoustic wave frequency $f = 40$ MHz with $L = 1.0$ cm, one can calculate $Q \approx 10$ that confirms the Bragg character of light scattering in the regime selected within the visible range of the light spectrum. Then, to estimate the frequency bandwidth of acousto-optical interaction with one-, two-, and three-phonon mechanisms of light scattering, one can use Eqs. (13b), (18b), and (21b) with the above-mentioned substitution of the angle $\delta\varphi = V/(Lf)$ by the enlarged value of $\delta\varphi_E = 25.6\delta\varphi$ due to the contribution from the acoustic anisotropy. Thus, one can write

$$\begin{aligned} \text{(a)} \quad \Delta f_0 &\approx 2V\sqrt{2n_0\zeta\lambda^{-1}\delta\varphi_E}, \\ \text{(b)} \quad \Delta f_2 &\approx \frac{n_0V}{2\lambda}\delta\varphi_E, \\ \text{(c)} \quad \Delta f_3 &\approx \frac{n_0V}{3\lambda}\delta\varphi_E. \end{aligned} \quad (34)$$

Strongly speaking, Eq. (21b) had been derived in Section 5 for the ratio $q = 0.866$. Nevertheless, the plots obtained via computer simulations show that Eq. (34c), following from Eq. (21b), is acceptable in the first approximation for estimating the frequency bandwidth of a three-phonon light scattering with the ratio $q = 1.936$ as well, see Section 5. In the case of using Eqs. (13b), (18b), and (21b) directly, i.e. with $\delta\varphi \approx 10^{-3}$ rad, the following set of values can be obtained: $\Delta f_0 \approx 33$ MHz at $\lambda = 633$ nm, $\Delta f_2 \approx 1.4$ MHz at $\lambda = 488$ nm, and $\Delta f_3 \approx 1.2$ MHz at $\lambda = 442$ nm. By contrast, the numerical estimations, based on Eq. (34), give the set $\Delta f_0 \approx 167$ MHz at $\lambda = 633$ nm, $\Delta f_2 \approx 36$ MHz at $\lambda = 488$ nm, and $\Delta f_3 \approx 28$ MHz at $\lambda = 442$ nm. Practically, of course, both these sets of data should be considered only as a lower and upper limit of bandwidths, respectively, for acousto-optical processes

under analysis, because the first set does not include acoustic anisotropy, while the second one does not take into account a number of restricting external factors. Nevertheless, Eqs. (34) predict that the contributions caused by the acoustic anisotropy are able to enlarge the frequency bandwidth of acousto-optical interaction in comparison with the case of pure acoustic diffraction.

Our experimental studies consisted of two parts. The first one included measuring the bandwidths of acousto-optical interaction in the regimes of a one-, two-, and three-phonon light scattering. The general schematic arrangement of the corresponding setup for these measurements is presented in Fig. 9. Lasers with three different wavelengths (i.e. with the red, light-blue, and deep-blue lines) were exploited to observe a triplet of the wide-band intensity–frequency distributions depicted in Fig. 10. A set of values recorded during these experiments with the same TeO_2 -cell includes $\Delta f_0 \approx 31$ MHz at $\lambda = 633$ nm, $\Delta f_2 \approx 16$ MHz at $\lambda = 448$ nm, and $\Delta f_3 \approx 4.5$ MHz at $\lambda = 442$ nm.

Let us discuss these data. The measured acousto-optic bandwidth $\Delta f_0 \approx 31$ MHz is close to estimation without the acoustic anisotropy. Moreover, the value of $\Delta f_0 \approx 31$ MHz represents approximately an octave at the central frequency 60 MHz, see Fig. 10a. Most likely, two these facts mean that the acousto-optical bandwidth Δf_0 is mainly determined by the bandwidths of the piezoelectric transducer by itself, so that acoustic anisotropy has no chance to manifest itself in the regime of a one-phonon anomalous light scattering. The restriction appearing from the transducer covers the effect of acoustic anisotropy, and that is why the experimental value of 31 MHz is too close to the numerical estimation of 33 MHz from Eq. (13b). At the same time, the measured acousto-optical bandwidths $\Delta f_2 \approx 16$ MHz and $\Delta f_3 \approx 4.5$ MHz are rather far from both the above estimations, see Figs. 10b and c. Because all these measurements had been done with the same acousto-optical cell, it is unlikely that influence of the piezoelectric transducer took place in the last two cases. Undoubtedly, we are meeting here the contribution of acoustic anisotropy. However, together with broadening the bandwidth due to that anisotropy, the other physical factor exists, which has the restricting effect. Evidently, such a physical factor consists in the effect mentioned at

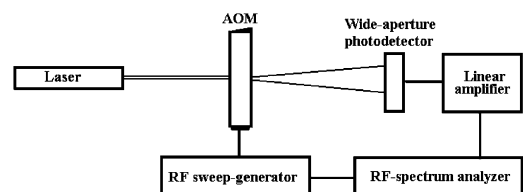


Fig. 9. General schematic arrangement for measuring the frequency bandwidths of a TeO_2 modulator in various regimes of multi-phonon light scattering.

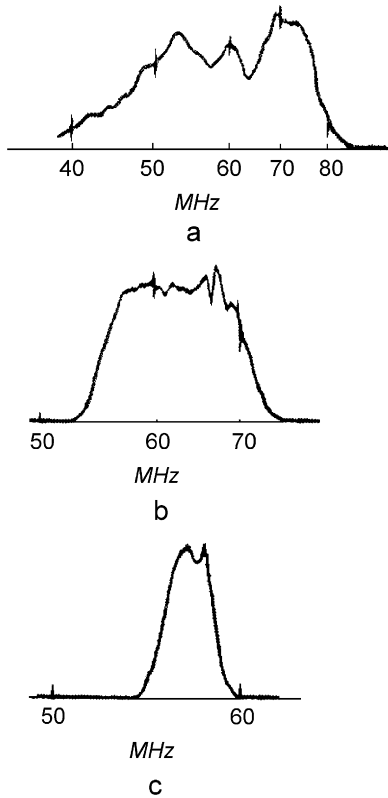


Fig. 10. Intensity–frequency distributions for one-phonon (a), two-phonon (b), and three-phonon (c) light scattering processes in a tellurium dioxide single crystal.

the end of Section 6. This effect is connected with varying the wave vectors on the diagrams in Figs. 1c and d, because it is ultimately conditioned by the necessity of meeting the conservation laws at all the intermediate stages of multi-phonon light scattering. That is why a contribution from the acoustic anisotropy is not able to exhibit itself by the full measure, and experimentally one can observe a sort of balance between the contributions inherent in anisotropic spreading of the acoustic beam and approximate fulfilling of the conservation laws in intermediate stages.

The second part of our experiments was related to estimating the possible resolution of modulators under consideration. In fact, the intensity distributions of an individual spot in the focal plane of the integrating lens for a multi-phonon light scattering in a TeO₂ acousto-optical modulator had been studied. In so doing, the experimental setup was re-arranged at the scheme shown in Fig. 11, where the technique, which had long been in use, with a scanning very narrow slit diaphragm was applied to our needs. This technique gives an opportunity to fix the continuous distribution of light intensity in the lobes of an individual spot really carefully in a rather wide dynamic range of about 25 dB. In parallel, the corresponding numerical estimations have been carried out to provide the possibility of their comparison

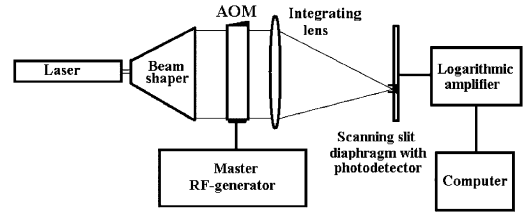


Fig. 11. General schematic arrangement for measuring the intensity profile of an individual spot.

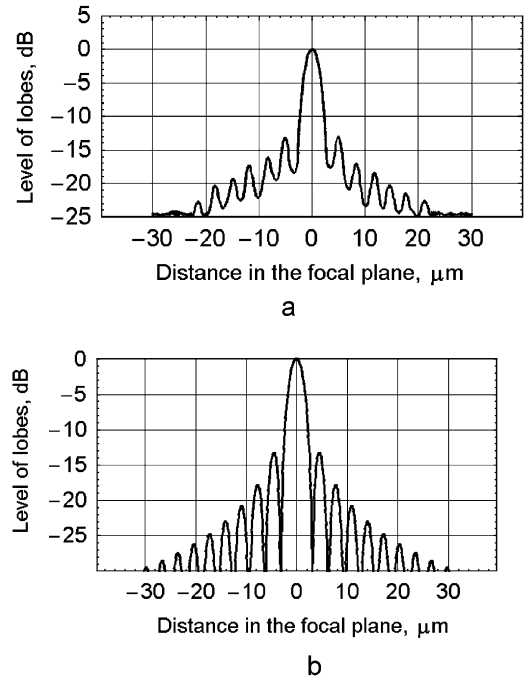


Fig. 12. Intensity distributions of an individual spot in the focal plane of the integrating lens for a two-phonon light scattering in a TeO₂ acousto-optical modulator: (a) experimental plot; (b) numerical simulation.

with the experimental data obtained. The fulfilled measurements have shown an expected result that the intensity distributions of individual spots, corresponding to the regimes of a one-, two-, and three-phonon light scattering, are very similar to each other. Such a result is caused by the fact that the angles of light scattering in these regimes do not exceed a few degrees in the case of a TeO₂ acousto-optical modulator, so that conditions for a one-, two-, or three-fold scattering of light are almost the same; mainly, they are determined by optical quality of a crystal and homogeneity of the acoustic beam inside the modulator. That is why only one example of the intensity distributions at an individual spot, related to a two-fold light scattering, is presented in Fig. 12a; the plot obtained from numerical estimation at the same conditions is displayed in Fig. 12b. One can see that the measured level of the first lobes lies at a level of around –13 dB with initially

homogeneous lighting of the modulator's aperture, which is in good coincidence with the well-known theoretical prediction [13] and looks rather acceptable practically from the viewpoint of application of a multi-phonon light scattering to spectral analysis of radio-wave and optical signals.

9. Conclusion

We have updated and developed a special approach to the Bragg scattering of light in optically anisotropic crystals marked by the inclusion of multi-phonon processes. In particular, the configurations related to one-, two-, and three-phonon scattering processes have been analyzed in detail to highlight both the frequency bandwidth and potential resolution inherent in optical modulators operating over a multi-fold light scattering. Because one-, two- and three-phonon processes provide the possibilities of realizing 100% efficiency within light scattering in the corresponding regimes, possible applications of these processes lie in implementing the optical modulators with rather large optical and acoustical aperture. That is why we have investigated the problems of optimizing the frequency bandwidths and potential resolution of such modulators. In so doing, we have included into consideration the contribution of the acoustic anisotropy of a cell's crystalline material. The analytical results have been confirmed by computer simulations and successfully compared with proof-of-principle data obtained during the experiments with a multi-phonon light scattering in a tellurium dioxide crystalline cell.

Acknowledgments

This work was financially supported by the CON-ACyT (Mexico), Projects # 41998-F and # 61237-F. The

authors thank Dr. N. Korneev (INAOE, Mexico) for fruitful discussion related to the mathematical description of acoustic anisotropy.

References

- [1] A.S. Shcherbakov, A. Aguirre Lopez, Binary encoded modulation of light based on collinear three-wave acousto-optical coupled states, *J. Opt. A: Pure Appl. Opt.* 5 (2003) 471–477.
- [2] A.S. Shcherbakov, A. Aguirre Lopez, Wave multiplication of binary encoded data exploiting solitary multi-pulse non-collinear three-wave coupled states, *J. Opt. A: Pure Appl. Opt.* 8 (2005) 464–472.
- [3] A.S. Shcherbakov, A. Aguirre Lopez, Shaping the optical components of solitary three-wave weakly coupled states in a two-mode waveguide, *Opt. Express* 11 (2003) 1643–1649.
- [4] V.I. Balakshy, V.N. Parygin, L.E. Chirkov, *Physical Principles of Acousto-Optics*, Radio i Svyaz, Moscow, 1985.
- [5] A. Korpel, *Acousto-Optics*, Marcel Dekker, New York, 1997.
- [6] R.W. Dixon, Acoustic diffraction of light in anisotropic media, *IEEE J. Quantum Electron.* QE-3 (1967) 85–93.
- [7] A.S. Shcherbakov, A. Aguirre Lopez, Observation of the optical components inherent in multi-wave non-collinear acousto-optical coupled states, *Opt. Express* 10 (2002) 1398–1403.
- [8] R.W. Klein, B.D. Cook, A unified approach to ultrasonic light diffraction, *IEEE Trans. SU-14* (1967) 123–134.
- [9] P.A.M. Dirac, *The Principles of Quantum Mechanics*, fourth ed., Yeshiva University, New York, 1964 (Chapter 4).
- [10] N. Uchida, N. Niizeki, Acousto-optic deflection materials and techniques, *Proc. IEEE* 61 (1973) 1073–1092.
- [11] Y. Ohmashi, N. Uchida, N. Niizeki, Acoustic wave propagation in TeO₂ single crystal, *J. Acoust. Soc. Am.* 51 (1972) 164–168.
- [12] V.G. Dmitriev, G.G. Gurzadyan, D.N. Wikogosyan, *Handbook of Nonlinear Optical Crystals*, Springer, New York, 1999.
- [13] J.W. Goodman, *Introduction to Fourier Optics*, second ed., McGraw-Hill, New York, 1996 (Chapter 4).